Chemical Imaging using Energy Filtered X-ray Photoemission Electron Microscopy

Kiyotaka Asakura[1], Takeshi Miyamoto[1], Hironobu Niimi[1], Shushi Suzuki[1]

[1] Catalysis Research Center, Hokkaido University, Sapporo, Japan

Introduction

Energy Filtered X-ray Photoemission electron microscopy (EXPEEM) is a technique to visualize the surface using X-ray-excited core-shell photoelectrons which have element specificity. We have developed a collinear type energy filter called as multipole Wien filter which can reduce the aberrations. Since the X-ray has a small radiation damage on materials, it is a good for the analysis of soft matters. We have shown the principle of the EXPEEM and its application to Ni_2P hydrodesulfurization catalyst surfaces.

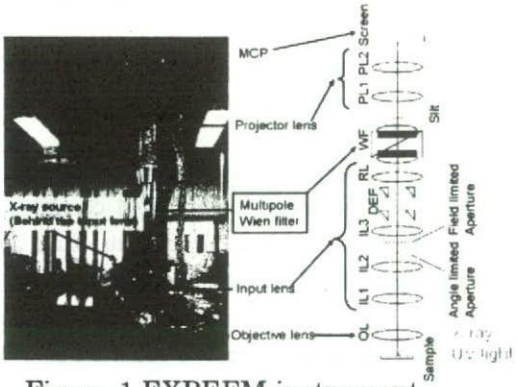

Figure 1 EXPEEM instrument

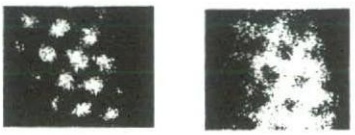

Fig.2 EXPEEM images (a) Au4f, (b)Ta 4f

Experimental setup

Figure 1 shows the EXPEEM machine. The sample was irradiated with X-ray. The ejected electro is collected by the objective lens and magnified by intermediate and projection lenses. The Energy analysis of photoelectron was carried out by a newly-developed multipole Wien filter which can reduce upto 3rd order abbreviations.

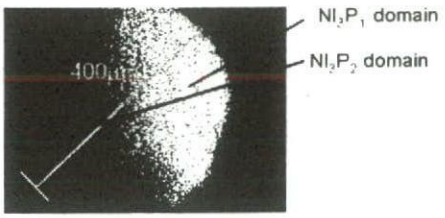

Fig.3 EXPEEM image of $Ni_2P(0001)$ surface

Results

Figure 2 shows the energy selected images of Au on Ta. Figure 2a gives the surface using Au4f peaks while Figure 2b shows the Ta 4f selected pictures. Figure 3 shows Ni_2P EXPEEM image excited using deuterium lamp. There are two equivalent surface structures on Ni_2P, i.e., Ni_3P and Ni_3P_2 the latter of which has a larger work function than the former and gives darker surfaces. What we observe is both surfaces are equally present on the surface of Ni_2P with a macroscopic size(a few hundred nm). This finding is important because Ni_3P which is regarded as a catalytically active center though it was believed thermodynamically instable. We are now conducting in-situ observation during the adsorption of H_2 ands thiophene.

Oral 1- 003

Formation of fine particles related with mechanical degradation of Ni-Ti superelastic alloys in biological fluids

Kenzo Asaoka[1] and Motohiro Uo[2]

[1] The University of Tokushima Graduate School, Institute of Health Biosciences, Department of Biomaterials & Bioengineering, 3-18-15 Kuramoto-cho, Tokushima, 770-8504, Tokushima, Japan

[2]Hokkaidou University, Graduate School of Dental Medicine, Department of Biomedical, Dental Materials & Engineering, Kita 13, Nishi 7, Kitaku, Sapporo 060-8586, Japan

Introduction

From retrieved Ni-Ti alloy used in orthodontic wire and retrieved titanium implant, we confirm that the alloy is naturally absorbed hydrogen in biological circumstances. To simulate hydrogen uptake of the alloy in biological fluid, hydrogen charging system was developed. Because hydrogen embrittlement of titanium alloys is known, effect of the superelastic deformation on hydrogen concentration in the alloys was experimentally determined, and confirmed the mechanical degradation related with hydrogen concentration. During charging of hydrogen to the alloys, hydride (TiNiH) was formed on the surface of the alloys, and nickel ion preferentially dissolved into the biological fluids. The dissolved ions were formed into metal hydroxide. We measured the distributions of the diameters of the fine particles, and discussed relationships between the number of particles and chemical composition related with the experimental conditions.

Materials and Methods

A commercial Ni-Ti superelastic alloy (55 mass% Ni-Ti) wire was used as specimens. The hydrogen charging of the specimens was conducted by cathodic electrolysis using a 0.9 % NaCl solution at a current density of 10 A/m^2 for 2 h at room temperature. The stress-strain curves of the charged alloys were measured. Distributions of fine particles in the solution after hydrogen charging were measured.

Results and Discussion

Hydrogen directly affects the metal structural degradation of superelastic Ni-Ti alloys. The functional deterioration of the alloys under physiological circumstances leads to low strength, brittleness, and short service life. The marked mechanical degradation by the hydrogen absorption is closely related with the sustaining stress/strain, phase of the alloys, and hydrogen distribution in the alloy. Elution of metal ions accelerates by hydrogen absorption, and formed corrosion products. The diameter of the fine particles in the solution was distributed from 100 nm to 100 μm. Those fine particles may be affected to the troubles of mucous membrane. These findings may be helpful to develop a new reliable medical device such as stents and catheter using of Ni-Ti superelastic/shape memory alloys.

Acknowledgements

This work was supported, in part, by the Grant from the Ministry of Health, Labor and Welfare of Japan.

Effect of temperature on crystallinity of carbonate apatite foam prepared from α-tricalcium phosphate by hydrothermal treatment

Akari Takeuchi[1], Melvin L. Munar[1], Hanae Wakae[1], Shigeki Matsuya[2], Kanji Tsuru[1], and Kunio Ishikawa[1]

[1] Department of Biomaterials, Faculty of Dental Science, Kyushu University, 3-1-1 Maidashi, Higashi-ku, Fukuoka 812-8582, Japan

[2]Section of Bioengineering, Department of Dental Engineering, Fukuoka Dental College 2-15-1 Tamura, Sawara-ku, Fukuoka 814-0193, Japan

Introduction. Carbonate apatite (CAP) foam with nano crystallite size and fully interconnected macroporous structure could be an ideal bone filler because it has quite similarity to cancellous bone in both inorganic chemical composition and morphology. Previously, we have reported that the CAP foam could be prepared from α-tricalcium phosphate (α-TCP) foam by the hydrothermal treatment with Na_2CO_3 at 200°C for 24 hrs [1]. However, the crystallinity of the CAP foam was much higher than that of bone which is consisted of nano crystallite CAP. In order to prepare CAP foam similar to cancellous bone in crystallinity as well as its inorganic composition and morphology, this study attempted to prepare CAP foam at lower temperature. Effect of hydrothermal temperature on crystallinity of CAP foam was investigated.

Materials and Methods. The α-TCP slurry was prepared by mixing the commercial α-TCP powder (α-TCP B, Taihei Chemical Co., Japan) and distilled water at a liquid to powder ratio of 9 mL/10 g. The polyurethane foam blocks with pore size of about 1 mm (HR-20D, Bridgestone, Tokyo, Japan) were impregnated with the slurry and the excess slurry was removed by compressed air. After drying at room temperature, the sponge with α-TCP powder was heated up to 400°C at 1°C/min to burn out polyurethane and subsequently heated to 1500°C and kept for 5 hrs. The sintered α-TCP foams were then immersed in 4 mol/L of Na_2CO_3 aqueous solution in Teflon vessel with stainless-steel jackets for the hydrothermal treatment, and kept at 100°C or 200°C for various periods up to 72 hrs. The foams before and after the hydrothermal treatment were characterized by X-ray diffraction (XRD), Fourier transform infrared (FT-IR) spectroscopy and scanning electron microscopy.

Results and Conclusion. The cancellous bone-like macroporous structure of α-TCP foam was maintained after the hydrothermal treatment. However, microscopic morphology of the foam frame significantly changed after the treatment for 72 hrs. Smooth surface of α-TCP foam was disappeared and the whole surface was covered with the plate-like deposits. Plate-like deposits observed after the treatment at 200°C had smooth surface whereas the deposits observed after the treatment at 100°C were constructed from spherical particles of approximately 200 nm in diameter. The results of XRD (Fig. 1) and FT-IR analysis showed that α-TCP was completely converted to CAP and the crystallinity was significantly lower than that of CAP prepared at 200°C. The XRD analysis also showed crystallite size of CAP prepared at 100°C was 42.2±0.6 nm. Hydrothermal treatment at 100°C allowed low-crystalline CAP foam whereas longer period was imposed for complete conversion of α-TCP foam into CAP foam.

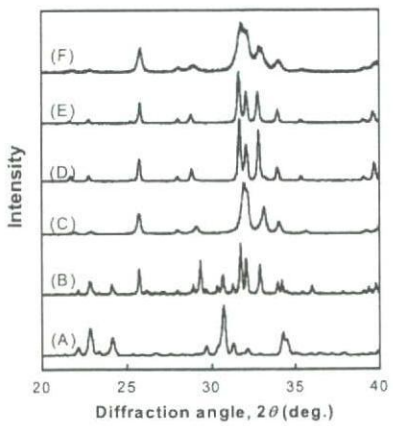

Fig. 1. XRD patterns of α-TCP powder (A) and specimen after hydrothermal treatment with Na_2CO_3 solution at 100°C for 24 hrs (B) or 72 hrs (C), and at 200°C for 24 hrs (D), hydroxyapatite (E), and biological apatite (F).

Reference.

[1] H. Wakae, A. Takeuchi, K. Udoh, S. Matsuya, M.L. Munar, R.Z. Legeros, A. Nakasima and K. Ishikawa: J Biomed Mater Res (2008) in press

Characterization of Electrical Properties of HL-60 Cell Membrane by Rotating of Cells Uptake of Nanoparticles in A DEP Chip

Cheng-Hsin Chuang*, Chen-Che Yeh

Department of Mechanical Engineering & Institute of Nanotechnology,

Southern Taiwan University, Tainan, Taiwan

Abstract

Electrorotation has become a very powerful diagnostic technique for measurement of dielectric properties of cells. However, only few papers investigated the electric-induced rotation of particles in a stationary alternating (AC) electric field instead of a rotating electric field. In this study, a microchip consisted of top grounded electrode, flow chamber and bottom chess-type electrode arrays to construct a stationary AC electric field for manipulation of cells by dielectrophoretic force as shown in the Fig. 1. Cells uptake of 13nm Au nanoparticles can easily rotated in the DEP chip as indicated in the Fig. 2. Besides of metal (Au) nanopartilces, we also introduced the dielectric (SiO2) nanoparticles for cells in order to study the effects of nanoparticles on electrorotation. As experimental results, both the percentage of cells in rotation and the range of rotational frequency for uptaken-Au-nanoparticles cells were higher and wider than the case of SiO2 nanoparticles, respectively. In addition, the membrane of a rotating cell could be deformed and broken after 30 to 40 minutes. In general, the electrorotation of cells can be attributed to the polarization and nonuniform distribution of nanoparticles within cells, shown in the Fig. 3; hence, the electrical properties of uptaken nanoparticles and the aggregation phenomenon have significant influences on resulting electrical torque. According to the rotational spectra (ROT), the membrane capacitance of HL-60 cells can be calculated in this method without a rotating electric field excited by poly-phase AC voltages.

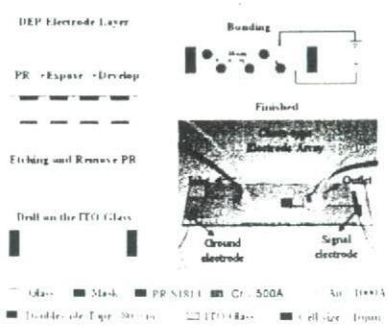

Fig. 1. The process flow for the fabrication of DEP chip.

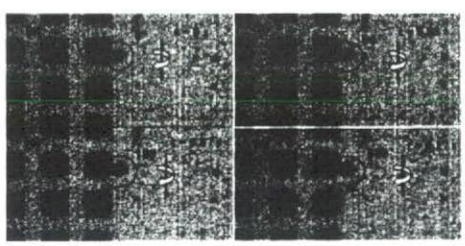

Fig. 2. The sequential OM pictures of one complete cycle as a single cell uptake of Au nanoparticles rotated in a nonuniform AC electric field with 10 V_{pp} and 100 KHz.

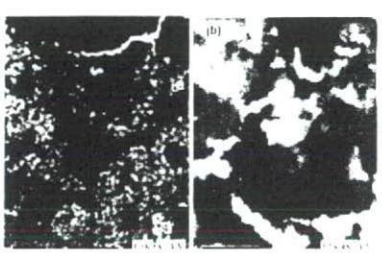

Fig. 3. TEM micrograph of single cell, (a) Au nanoparticles dispersed in cytoplasm and aggregated into larger particles about the size of 100~200nm; (b) SiO_2 nanoparticles not only aggregated into larger particles about the size of 200 ~ 300 nm but also attracted each other into 2~3 um clusters

Anti-bacterial Ceramics using Ag bearing Glaze

Norifumi Isu[1], Yoshihiro Kato[1], Satoru Yamazaki[1],
Atsushi Nakahira[2] and Chiya Numako[3]

[1] INAX Corp., 3-77 Minato Tokoname Aichi, 479-8588, Japan

[2] Osaka Prefecture University, 1-1 Gakuen, Nakaku, Sakai, Osaka, 599-8531, Japan

[3] The University of Tokushima, 1-1 Minami-josanjima, Tokushima 770-8502, Japan

Introduction

From the view point of healthy environment, anti-bacterial products become common. Among inorganic anti-bacterial agents, Ag is widely used because of high activity, broad anti-bacterial spectra, low toxic for human and durability. Anti-bacterial mechanism of metal is not well understood, but two hypotheses are suggested: one is dissolved ion theory and the other is reactive oxygen species theory. For the sanitary ware and tile, the anti-bacterial agent was added into the glaze (amorphous alminosilicate). The state of Ag elements in the glaze is very important to control anti-bacterial properties, but it was difficult to determine because of low concentration and the presence of interference elements. The purpose of this investigation was to examine the state of Ag and Zn in the glaze of anti-bacterial ceramics by using X-ray absorption fine structure (XAFS) analysis.

Results and Discussion

Anti-bacterial ceramic samples were prepared by the same way of actual products. Plate shape green body was fabricated by slip casting followed by drying. Glaze and Ag containing suspension was sprayed on the surface of green body, followed by sintering at 1200°C in the air. The Ag-glaze layer of the anti-bacterial ceramic was amorphous aluminosilicate with the 500□m thickness containing 0.08 mass% Ag_2O. XAFS measurements were carried out at room temperature in the air. Ag K-edge XAFS measurements were performed at BL01B1 line, SPring-8. A Si(111) double crystal monochromator was used with 8GeV electron storage ring. Antibacterial activities of Ag-glaze was confirmed by the growth of *Staphylococcus aureus*.

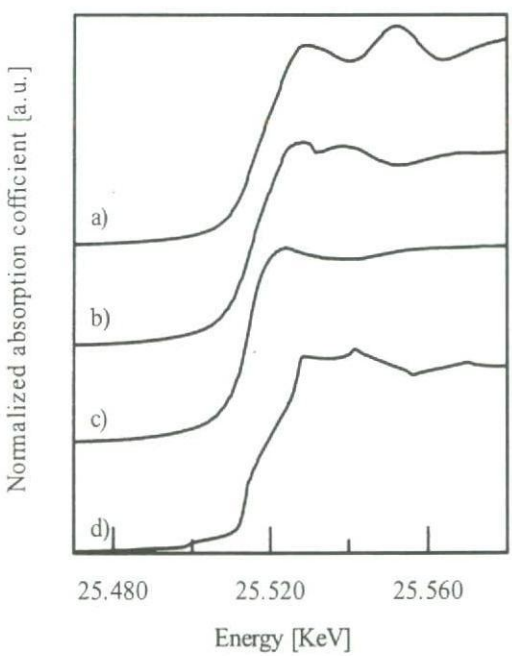

Fig.1. Normalized Ag K-edge XANES spectra for (a) Ag metal, (b) Ag_2O, (c) Ag-glaze, (d) AgO.

The XANES spectrum of Ag-glaze was similar to that of Ag_2O, indicating that major components of Ag in the glaze existed as monovalent (Fig. 1). From the fourier transforms, Ag-glaze had only one peak at 1.6Å attributed to Ag-O bonding, and Ag-Ag interaction was not observed. In comparison with Ag_2O, Ag-O bond length of Ag-glaze was slightly increased. These results indicated that Ag atoms in the Ag-glaze were isolated from crystal structure.

Effective hydrogen generation using stratified type photocatalyst

Hideyuki Takahashi

Graduated School of Environmental Studies, Tohoku Univ,

6-6-20, Aoba, Aramaki, Aoba-ku, Sendai 980-8579, Japan

Many researchers reported that natural energy should be utilized for the human life because of the depletion of fossil fuel and also the environmental problem. Among the various methods to utilizing the natural energy, photocatalytic decomposition of hydrogen sulfide (H_2S) is considered as an efficient alternative route to produce new energy (hydrogen) compared with the splitting of water because of its low potential. Moreover, decomposition of H_2S by using solar energy and photocatalyst may gives us the candidate for the resolution of environmental problems, since quite large amounts of energy was consumed for the decomposition of H_2S which evolved from the distillation of fossil fuel. Among various semiconductor materials, only the sulfide type photocatalyst can act stably in the H_2S solution, while metallic and/or oxide type photocatalyst is sulfurized. Recently, we reported that the synthesis of CdS and ZnS nano-sized capsule which had the gradient metal concentration in its wall, called as "stratified type photocatalyst", and demonstrated that these materials showed the high photocatalytic activities for the decomposition of H_2S. Thus, it can be said that photocatalytic decomposition of H_2S into H_2 by using the stratified type photocatalyst is considered as efficient route for the conversion of natural energy (solar energy) into clean energy (H_2). Here, we should consider the reaction route for the hydrogen generation from hydrogen sulfide. H_2S gas can be dissolved into basic aqueous solution as follows;

$$H_2S \rightarrow HS^- + H^+$$

Photodecomposition of HS^- ion was obeyed to the following formula;

$$2HS^- \rightarrow 2H^+ + S_2^{2-} + 2e^-$$

$$2H^+ + 2e^- \rightarrow H_2\uparrow$$

These formulas illustrated that this reaction route was "one way" like carbon cycle. Therefore, to construct the new energy generation system based on the utilizing natural energy, effective conversion route from S_2^{2-} ion into H_2S gas by using natural energy should be developed. In this study, effective conversion route utilizing the bio reaction will be introduced. By using bio reactor, evolved gas contained the various gases, such as methane and CO_2. Therefore, H_2S gas should be purified. Moreover, poly sulfide ion (S_2^{2-} ion) is synthesized as the by-products during the reaction, consequently photocatalytic reaction rate is decreased with increasing these concentration in the solution. Thus, poly sulfide ion should be removed by the other methods; nevertheless it was not chemically adsorbed on the solid absorbent surface since its surface potential was negative in basic condition, such as pH13.

In my presentation, recent efforts to construct the sulfur cycle of our research group will be introduced.

Oral 1- 005

Nanotechnology policy on health and environment in Japan: An international comparison

Masami MATSUDA[1], Geoffrey HUNT[2]

[1] School of Nursing, University of Shizuoka, Yada, Suruga-ku, Shizuoka city, Japan

[2] Bioethics, St Mary's University College, Waldegrave Road, Twickenham, United Kingdom

Introduction The health and environmental impacts of the novel properties of substances that appear at nanoscale are mostly unknown and unpredictable. The conflict between the potential benefits and potential hazards of nanomaterials have to be understood in the context of converging global crises of energy, climate change and economic down-turn and the priority for new technologies of sustainability. Nanomaterials may have great benefits but some have the potential to damage skin, brain, liver and lung tissue, to be persistent in the environment, or to destroy ecologically essential micro-organisms. Nanoparticles have been described as 'Janus-faced', that is, having two sides[1]. When a nanomaterial starts to cause widespread damage then not only are consumers and citizens harmed but there will be long legal and regulatory battles, costly efforts, and painful public-relations exercises.

Precautionary principle Since there are few scientific facts on the risk of nanomaterials, we need to apply the precautionary principle as a societal policy. It makes no sense to proceed with mass production of applications on the basis that 'there is no evidence of harm', when so little effort has yet been made to gather such evidence. In Japan the importance of complying with a global precautionary approach is not well understood nor is the government policy process well equipped compared with the UK, EU and US. When there is an adequate body of knowledge on the characteristics of nanomaterials we shall need a methodology to provide standards and limits. This would minimize 'false positives' and 'false negatives' during implementation of policies for nanotechnology applications.

UK government report In the UK, DEFRA published its second research report in Dec. 2007 'Characterising the Potential Risks posed by Engineered Nanoparticles[2]. DEFRA urges that more attention is paid to the development of appropriate hazard and risk methods[3] and to the accumulating body of toxicological evidence.

Recent toxicology studies We review some recent seminal papers from the new journal[4]. Hypotheses are now being tested that some nanoparticles may harm specific biological systems, such as inflammatory mechanisms, the hormonal system and gene expression dynamics. We summarize useful review papers[5,6].

Conclusions Besides the technical methodologies for an adequate and effective nanotechnology policy, it is important to understand the cultural background, history, philosophy and governmental institutions.

Literature References

[1] K Donaldson and A Seaton:The Janus faces of nanoparticles. J Nanosci Nanotechnol 7(12)(2007),p.4607

[2] A Helland, et al.:Risk assessment of engineered nanomaterials Environ Sci Technol. 42(2)(2008),p. 640.

[3] DEFRA, Nanotechnology Report, London.www.defra.gov.uk/ENVIRONMENT/nanotech/index.htm(2008)

[4] A.K. Jain et al.: Carbon nanotubes and their toxicity, Nanotoxicology. 1(3) (2008),p.167.

[5] M.E. McAuliffe; M. J. Perry: Are nanoparticles potential male reproductive toxicants? Nanotoxicology. 1(3) (2008),p.204.

[6] V.H. Grassian.et al.: Inflammatory response of mice to manufactured titanium dioxide nanoparticles. Nanotoxicology. 1(3) (2008),p.211.

Development of International Standard for measurement methods for the characterization of multi wall carbon nanotube

Fuminori Munekane[1], Kazuyoshi Furuta[2]

[1]600 Tanaka-cho, Akishima-shi, Tokyo 196-8522 Japan

[2]1-8 Nakase, Mihama-ku, Chiba-shi, Chiba 261-8507 Japan

ISO/TC229 was established in 2005 for developing International Standard which concerns to nanotechnologies. This committee consists of three working groups, JWG1 (Terminology and Nomenclature), JWG2 (Measurement and Characterization) and WG3 (Environment, Health and Safety). JWG1 and JWG2 are joint working groups with IEC/TC113 (Nano Electronics).

The scope of JWG2 (Measurement and Characterization) is the development of standards for measurement, characterization and test methods for nanotechnologies, taking into consideration needs for metrology and reference materials. Now there are ten working items and almost items concern to carbon nanotube.

Author is developing technical specification (TS) of measurement methods for the characterization of multi wall carbon nanotube as a project leader. This TS consists of three categories, that is purity, physical properties and geometrical properties. As purity is important for the study of environment, health and safety as well as business, the items concerning to purity are developed first as "part A". The purity category consists of seven items, that is moisture content, ash content, metallic constituent, volatile content, polyaromatic hydrocarbon content, carbon materials excluding MWCNTs, and disorder as following table.

Category	Property	Method	Part
Purity	Moisture content	Weight loss measurement (*)	A
Purity	Ash content	Weight loss measurement (*)	A
Purity	Metallic residual content	XRF or ICP-AES	A
Purity	Volatile content	Weight loss measurement (*)	A
Purity	Polyaromatic hydrocarbons	GC-MS	A
Purity	Carbon materials excluding	SEM and/or TEM	A
Purity	Disorder	Raman Spectroscopy	A
Physical properties	Burning properties	TG/DTA	A
Physical properties	Resiliency (Compression	Density and resiliency measurement (*)	B
Physical properties	Bulk Density	Bulk density measurement	B
Physical properties	Specific gravity	Pycnometer	B
Physical properties	Specific surface area	BET	B
Physical properties	Stacking nature	XRD or TEM	A
Physical properties	Electric resistivity	Volume resistivity measurement	B
Geometrical propert	Morphology	SEM and/or TEM	A
Geometrical propert	Inner diameter	TEM	A
Geometrical propert	Outer diameter	SEM and/or TEM	A
Geometrical propert	Length	SEM and/or TEM	A

Antimicrobial Activity of Fullerenes and Their Derivatives

Hisae Aoshima*[1], Ken Kokubo[2], Shogo Shirakawa[2], Masayuki Ito[1], Shuichi Yamana[1], and Takumi Oshima[2]

[1] Vitamin C60 BioResearch Corporation, Tatsunuma Tatemono Bldg., 9F, 1-3-19, Yaesu, Chuo-ku, Tokyo 103-0028, Japan.

[2] Division of Applied Chemistry, Graduate School of Engineering, Osaka University Suita, Osaka 565-0871, Japan.

In order to find the novel functionality of fullerenes in cosmetic industry, we have assessed their antioxidant activities [1]. In this study, antimicrobial activities of fullerene C_{60} and its derivatives against various bacteria and fungi were evaluated. The minimum inhibitory concentration (MIC) values were measured using an agar plate dilution method according to the Clinical and Laboratory Standard Institute. The fullerene samples tested were variously modified water-soluble C_{60} (PVP/C_{60}, γ-CD/C_{60} [1], and Nano-C_{60} [2]) and three fullerenols such as $C_{60}(OH)_{12}$, $C_{60}(OH)_{36}$•$8H_2O$, and $C_{60}(OH)_{44}$•$8H_2O$. Catechin was used as a reference material. Although pristine C_{60} showed no antimicrobial activity, fullerenols exhibited a good antimicrobial activity against *P. acnes*, *S. epidermidis*, *C. albicans*, and *M. furfur*. In particular, $C_{60}(OH)_{44}$ exhibited a strong and versatile antimicrobial activity comparable to catechin. These results indicate that the hydroxyl groups of fullerenes are responsible for the antimicrobial activity. It is expected that $C_{60}(OH)_{44}$ has a possible wide-ranging application in the field of the household goods as well as the cosmetic ingredients.

Table 1. Antimicrobial activity of various fullerene derivatives

Strain	MIC (μg/mL)				
	$C_{60}(OH)_{44}$	$C_{60}(OH)_{36}$	$C_{60}(OH)_{12}$	C_{60}[a]	(+)-Catechin
Escherichia coli	–[b]	–	–	–	5120
Bacillus species	–	–	–	–	5120
Staphylococcus aureus (MRSA)	2000	–	–	–	5120
Staphylococcus aureus (MSSA)	2000	–	–	–	5120
Staphylococcus epidermidis	2000	2000	–	–	2560
Propionibacterium acnes	1500	–	–	–	2560
Candida albicans	1200	600	3300	–	–
Malassezia furfur	900	1850	3750	–	37

[a] All PVP/C_{60}, γ-CD/C_{60}, and Nano-C_{60} were tested. [b] No antimicrobial activity (–) was observed.

[1] H. Takada, K. Kokubo, and T. Oshima, *Biosci. Biotecnol. Biochem.* Vol. *70* (2007), p.3088.

[2] S. Deguchi, S. Mukai, M. Tsudome, and K. Horikoshi, *Adv. Mater.* Vol. *18*, (2006), p.729.

Corresponding Author: Hisae Aoshima, E-mail: hisae.aoshima@vc60.com

Nanomedical Applications of Functionalized Carbon Nanotubes

Alberto Bianco

CNRS, Institut de Biologie Moléculaire et Cellulaire, Laboratoire d'Immunologie et Chimie Thérapeutiques, 15, Rue René Descartes, 67084 Strasbourg, France

The applications of carbon nanomaterials, including carbon nanotubes (CNTs), carbon nanohorns and nanodiamonds, in the emerging field of nanomedicine are intensifying [1,2]. CNTs hold a lot of promises on biomedical applications for different reasons: high stability, water solubility, lack of intrinsic immunogenicity, efficient payload capacity, and rapid cellular uptake [3]. The organic functionalization has facilitated the manipulation of this type of nanomaterial, thus opening the way to the potential use of CNTs as a novel vectors for drug delivery [4]. Functionalized CNTs can be considered as a promising alternative to the common drug delivery systems. In this context, we have explored the possibility of targeted delivery of small organic molecules (antibiotics and anticancer), peptides and nucleic acids [5,6]. In this presentation we will describe the functionalization and biomedical applications of carbon nanotubes loaded with different therapeutic agents. We will also address the critical issue of their toxicity [7].

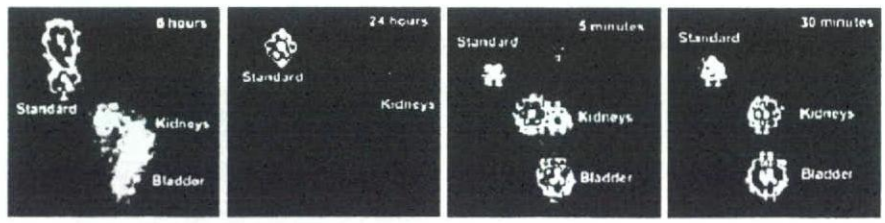

Figure. Biodistribution of radiolabeled CNTs after 5 min, 30 min, 6 h and 24 h post-injection.

Literature References

[1] A. Bianco, K. Kostarelos and M. Prato: Expt. Opin. Drug. Deliv. 5 (2008), p. 331

[2] M. Prato, K. Kostarelos and A. Bianco: Acc. Chem. Res. 41 (2008), p. 60

[3] K. Kostarelos, L. Lacerda, G. Pastorin, W. Wu, S. Wieckowski, J. Luangsivilay, S. Godefroy, D. Pantarotto, J.-P. Briand, S. Muller, M. Prato and A. Bianco: Nature Nanotech. 2, (2007), p. 108

[4] D. Tasis, N. Tagmatarchis, A. Bianco and M. Prato: Chem. Rev. 106 (2006), p. 1105.

[5] D. Pantarotto, R. Singh, D. McCarthy, M. Erhardt, J.-P. Briand, M. Prato, K. Kostarelos and A. Bianco: Angew. Chem. Int. Ed. 43 (2004), p. 5242

[6] W. Wu, S. Wieckowski, G. Pastorin, M. Benincasa, C. Klumpp, J.-P. Briand, R. Gennaro, M. Prato and A. Bianco: Angew. Chem. Int. Ed. 44 (2005), p. 6358

[7] L. Lacerda, A. Soundararajan, G. Pastorin, K. Al-Jamal, J. Turton, P. Frederik, M.A. Herrero, S. Li, A. Bao, D. Emfietzoglou, S. Mather; W.T. Phillips, M. Prato, A. Bianco, B. Goins and K. Kostarelos: Adv. Mater. 20 (2008), p.225

YR - 2

Electrode Arrays of Carbon Nanofibers for Biosensing at the Molecular and Cellular Level

Jessica Koehne[1,4], Hua Chen[2], Alan Cassell[3], Gang-yu Liu[4], Jun Li[5] and M. Meyyappan[1]

[1]NASA Ames Research Center, Moffett Field, CA 94035, USA
[2]ELORET Corporation, Moffett Field, CA 94035, USA
[3]UARC, University of California Santa Cruz, Moffett Field, CA 94035, USA
[4]Department of Chemistry, University of California Davis, One Shields Ave, Davis, CA 95616, USA
[5]Department of Chemistry, Kansas State University, 111 Willard Hall, Manhattan, KS 66506 USA

Carbon nanofibers (CNFs) are highly conductive and robust materials with high aspect ratios. Their unique properties and intriguing nanostructure can be employed to develop new tools to interrogate biomolecules and cells at nanoscale. Here, we report two studies using vertically aligned CNFs. First, a reliable nanoelectrode array (NEA) based on vertically aligned CNFs embedded in SiO_2 is used for ultrasensitive DNA detection, shown in Fig. 1a. Characteristic nanoelectrode behavior is observed using low-density CNF arrays for measuring both bulk and surface immobilized redox species such as $K_4Fe(CN)_6$ and ferrocene derivatives [1]. The open-end of CNFs presents similar properties as graphite edge-plane electrodes with wide potential window, flexible chemical functionalities, and good biocompatibility [2,3]. Oligonucleotide probes are selectively functionalized at the open ends of the nanotube array and specifically hybridized with oligonucleotide targets. The guanine groups are employed as the signal moieties in the electrochemical measurements. $Ru(bpy)_3^{2+}$ mediator is used to further amplify the guanine oxidation signal. The hybridization of subattomoles of PCR amplified DNA targets is detected electrochemically by combining the MWNT nanoelectrode array with the $Ru(bpy)_3^{2+}$ amplification mechanism [4]. Second, the SiO_2 matrix was etched back using a plasma process to produce needle-like protruding nanoelectrode arrays. This platform can be used towards biosensing at the single cell level by penetrating fibers into cells for investigating gene transfection, electrical stimulation, and detection of cellular processes, shown in Fig. 1b. Extensive confocal microscopy measurements will be present to verify the viability of PC12 neural cells upon CNF impaling, as well as determining the location of CNF. Our goal is to take the advantage the nanostructure of the CNF arrays for unconventional biomolecular studies requiring ultrahigh sensitivity, high-degree of miniaturization, and selective biofunctionalization.

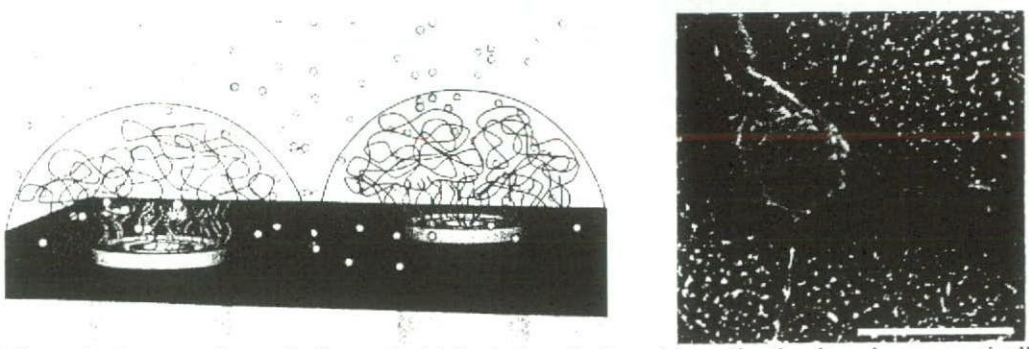

Figure 1: Images of two platforms for biological analysis and investigation based upon vertically aligned carbon nanofibers. a) SiO_2 embedded CNFs act as ultramicroelectrodes for ultrasensitive DNA detection. b) Needle-like protruding CNFs act as penetrating probes for cellular analysis, scale = 8 μm.

References

[1] J. Li, H. T. Ng, A. Cassell, W. Fan, H. Chen, Q. Ye, J. Koehne, J. Han, M. Meyyappan: NanoLett. Vol. 3, (2003), p. 597.

[2] L. McCreery, in *Electroanalytical Chemistry*, ed. A. J. Bard, Marcel Dekker, Inc., New York, 1991, Vol. 17, p 221.

[3] J. Koehne, J. Li, A. M. Cassell, H. Chen., Q. Ye, H. T. Ng, J. Han, M. Meyyappan: J. Mat. Chem. Vol. 14 (2004), p. 676.

[4] J. Koehne, H. Chen, J. Li, A. Cassell, Q. Ye, H. T. Ng, J. Han, M. Meyyappan: Nanotech. Vol. 14 (2003), 1239.

Biomimetic nerve guidance grafts: Synergism of physical nano-topography and biochemical guidance cues

Hui Shan Koh[1], Thomas Yong[2], Casey K Chan[2,3], Seeram Ramakrishna[1,2,4]

[1]NUS Graduate School for Integrative Sciences and Engineering, [2]Division of Bioengineering, [3]Department of Orthopaedic Surgery, [4]Department of Mechanical Engineering
9 Engineering Drive 1, National University of Singapore, Singapore

Introduction

Guidance of axonal outgrowth to the appropriate innervating target during development is known to be influenced by haptotactic cue that includes ECM proteins. Nanofiber alignment [1] and modification of nanofibers with biochemical proteins [2] are hypothesized to enhance nerve regeneration in rat sciatic nerve injury repair. By controlling the processing parameters and experimental set-up, nanofiber morphology and alignment can be achieved to create an ECM-like environment to enhance nerve regeneration.

Materials and Methods

Blended electrospinning (Fig. 1) was employed to produce nanofibrous ECM coupled poly(L-lactide) (PLLA) membranes and nerve grafts. Blended laminin-PLLA and collagen-PLLA nanofibers were prepared by uniformly mixing laminin and collagen at a ratio of 4 μg and 120 μg with 1 mg of PLLA, respectively, in 1,1,1,3,3,3-hexafluoro-2-propanol (HFP). High electrospinning voltages were applied at 10 kV, 18 kV and 10 kV DC for PLLA, blended laminin-PLLA and blended collagen-PLLA nanofibrous membrane respectively. To fabricate nerve grafts, a rotating mandrel was used as the collector.

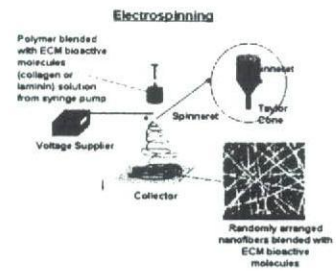

Fig. 1. Blended electrospinning of biomimetic nanofibers.

Results and Discussion

Polymeric nerve graft (Fig. 2) made of PLLA has been successfully fabricated that is biological and mechanically reliable (Table 1). These nanofibrous nerve graft has micro-porous architectures that can facilitate the transport of diffusible biomolecules to aid in nerve regeneration (Table 1).

Fig. 2. Scanning electron microscopy images of PLLA nanofibrous nerve graft.

Pore size (μm)	Ultimate tensile strength (kPa)$^+$	Ultimate tensile strain (%)$^+$	Young's Modulus (MPa)$^+$
1.19 ± 0.50	1990 ± 250	39 ± 18	61.8 ± 2.6

Table 1. Mechanical properties electrospun PLLA nerve graft ($^+$ Mechanical test on nanofiber sheet).

Furthermore, extracellular matrix bioactive molecules such as laminin and collagen type-I that can accelerate axonal outgrowth were coupled onto PLLA nanofibers using blended electrospinning (Table 2). Neural cells cultured on ECM-polymer nanofibers showed enhanced *in vitro* cell viability and neurite outgrowth (results not shown here). Preliminary analysis of *in vivo* study shows promising results using these synergistic nano-topographical and biochemical polymer nerve grafts to repair rat nerve injury.

Materials	PLLA nanofibers	PLLA-collagen nanofibers	PLLA-laminin nanofibers
Atomic Force Microscopy Image			
Nanofiber diameter (nm)	470 ± 170	240 ± 110	130 ± 40
Surface roughness (nm)	590 ± 18	440 ± 37	290 ± 41

Table 2. Analysis of surface roughness of ECM-PLLA nanofibers.

References

[1] F. Yang, R. Murugan, S. Wang and S. Ramakrishna: Biomaterials Vol. 26 (2005), p. 2603
[2] M. TessierLavigne and C.S. Goodman: Science Vol. 274 (1996), p. 1123

Gene expression analyses of human macrophage phagocytizing sub-μ titanium particles by allergy DNA chip (Genopal™)

M. TAIRA[1], T. NEZU[1], M. SASAKI[2], S. KIMURA[2],

T. KAGIYA[3], H. HARADA[3], T. NARUSHIMA[4], Y. ARAKI[1]

Departments of [1]Dental Materials Science and Technology, [2]Oral Microbiology and [3]Oral Anatomy II, Iwate Medical University School of Dentistry, Morioka, Japan, and [4]Department of Materials Processing, Graduate School of Engineering, Tohoku University, Sendai, Japan

Objectives: Both titanium (Ti) wear debris and lipopolysaccharide (LPS, endotoxin of gram-negative bacteria) cause macrophage to produce inflammatory cytokines, leading to osteolysis. The purpose of this study was to examine gene expressions of human macrophage phagocytizing sub-μ Ti particles by allergy DNA chip.

Materials and methods: Human monocytic cell line THP-1 ($1x10^8$) was differentiated into macrophage by culturing for 2 days in RPMI1640 medium (10 ml) supplemented with 10% fetal bovine serum and 200 nM phorbol-12-myristate-13-acetate (PMA) on four culture dishes at 37 degree C in a humidified 5% CO_2 atmosphere, and old media were exchanged with four media such as the supplemented RPMI 1640 without PMA (Control), that with 1.0 μg/ml *Esherichia coli* O26 LPS (LPS (+)), that with suspended sub-μ Ti particles (0.5 wt%, Koujyundo Kagaku, Tokyo, Japan) (SMT), and that with LPS and Ti particles (LPS (+) SMT). After 6 hours' culture, total RNA were extracted with Trizol™ (Invitrogen, Carlsbad, CA, U.S.A.), and then gene expressions were evaluated by DNA allergy chip (Genopal™, Mitsubishi Rayon, Tokyo, Japan) with 295 allergy and inflammation related genes.

Results and discussion: We found that several genes were significantly up-regulated by LPS and phagocytosis of sub-μ Ti particles, such as those of three inflammatory cytokines (TNF, IL1B, IL6) and the inflammation-mediated transcription factor (NFKB1) as indicated in Table 1. It was speculated that LPS and phagocytosis of sub-μ Ti particles might activate signaling pathways through NFKB1 (e.g. Toll-like-receptor and MAPK pathways) so that downstream genes of TNF, IL1B and IL6 as well as IL8, CCL1 and CD44 were significantly up-regulated. Blockage of NFKB1 may prevent the inflammation.

Table 1 Gene expression values of the macrophage

Medium	Gene name						
	TNF superfamily	IL1B	IL6	IL8	CCL1	CD44	NFKB1
Control	166	1590	62	425	117	1762	509
LPS (+)	784	14473	247	13455	3129	3726	1413
SMT	409	14409	115	8294	1262	3948	1219
LPS (+) SMT	828	20586	365	20584	2500	4551	1744

Identification and assessment of the effects of engineered nanoparticles on brain cells

M. Iwe[1], A. Springer[2], S. Bastian[1], T. Meissner, A. Potthoff, V. Richter, H. Ikonomidou[1], W. Pompe[2], M. Gelinsky[2]

[1]Department of Pediatric Neurology, University Children's Hospital, Technical University Dresden, Fetscher Str. 74, D-01307 Dresden, Germany

[2]Max Bergmann Center of Biomaterials, Technical University Dresden, Institute of Materials Science, Budapester Str. 27, D-01069 Dresden, Germany

The use of synthetic nanoparticles is of increasing interest but limited information about their interaction with cells exists. In the framework of a cooperative project, funded by the German Federal Ministry of Education and Research, we are investigating the effects of these technically relevant nanoparticles (NP) on cells, using physicochemical, biochemical and molecular biological methods as well as microscopical techniques. In detail, we are quantifying alteration of cell attachment and proliferation by NP, investigating cytotoxicity, characterizing changes of the mitochondrial membrane potential and of cell morphology due to interaction with NP by means of SEM, TEM and fluorescence microscopy. In addition, we want to examine the uptake and distribution of the NP inside the cells. Cell culture systems in this project include several cell types like like CaCo 2, HaCaT and A459. *In vivo* studies have shown that NP can be found within the brain of exposed animals. Therefore, we are also using primary neuronal cultures and primary glial cultures of the rat brain and OLN 93 (oligodendrocyte precursor rat cell line). Here we are focusing only on the effects of NP on brain cells. So far we have assessed the effects of tungsten carbide (WC) and tungsten carbide cobalt (WC-Co) NP which are released during the manufacturing process of cutting tools, and single-walled carbon nanotubes (SWCNT) which are of growing interest for technical and medical applications. The cell cultures were exposed to well characterized and stable suspensions of these particles in a time and concentration dependent manner. Many NP tend to aggregate when they are suspended in aqueous media. We demonstrated that the WC NP are stabilised over a period of several days in cell culture medium containing 10% foetal calf serum. To identify whether cell toxicity occurs, we applied in a first step different *in vitro* viability and cytotoxicity assays. The results show that WC NP are less toxic than WC-Co NP and SWCNT in glial cells. Viability of neurons was not or only slightly influenced. Depending on the time point of exposure the cells showed different degrees of compromise in adhesion. Treatment with SWCNT and WC-Co also caused a change of the mitochondrial membrane potential. With SEM as well as TEM we observed, that the NP passed the outer cell membrane but were not found within the nuclei. Decreased viability and proliferation as well as reduced adhesion of brain cells suggest that NP interfere with the function of cells of the central nervous system.

Unexpected immunological response against sterically stabilized, PEGylated, liposome after intravenous injection.

Tatsuhiro Ishida and Hiroshi Kiwada

Institute of Health Biosciences, Department of Pharmacokinetics and Biopharmaceutics, the University of Tokushima, 1-78-1 Sho-machi, Tokushima 770-8505, Japan

Drug carrier systems are being developed in order to achieve reduction in undesired side effects and to increase therapeutic efficacy of a drug by controlling its biological disposition in the body. Nano-drug carrier systems such as liposomes have been extensively investigated and several formulations have been already approved or are under clinical trials all over the world. The main problem in the development of nano-drug delivery systems was their rapid clearance from blood circulation and consequently sub-optimal delivery of the active ingredient to the target tissue or organ. Nowadays, drug carriers are usually coated with a hydrophilic polymer such as polyethylene glycol (PEG). It is generally believed that the polymer coating diminishes interactions with serum proteins such as opsonins and thus recognition by cells of mononuclear phagocyte system, resulting in prolonged circulation half-lives. The most successful example of a nano-carrier system for clinical use, exploiting polymer-coating technology, are the doxorubicin-containing sterically stabilized liposomes (PEGylated liposomes), known under the commercial name Doxil/Caelyx. However, several researchers including ourselves, showed evidence that unexpected immune responses may occur even to such polymer-coated nano-carriers. This illustrates that the processes governing the interaction of the carrier with the biological milieu following parenteral administration are still largely unclear. An interesting phenomenon which has recently been observed in our laboratory concerns an unexpected change in pharmacokinetic behavior of PEGylated liposomes when they are given to identical rat. When administered within a certain interval, a second dose of PEGylated liposomes extensively accumulated in liver as a result of taken up by Kupffer cells, resulting in rapid clearance from the blood circulation (referred as to the accelerated blood clearance (ABC) phenomenon). We found that anti-PEG IgM produced in response to first dose PEGylated liposomes and the subsequent complement activation triggered by binding the IgM to second dose resulted in the accelerated clearance and enhanced hepatic uptake of the second dose PEGylated liposomes. So far, we have provided some evidence that unexpected immune responses occur when nano-drug carriers are introduced into the animal body. Under certain conditions such immune responses conceivably occur in humans as well and thus produce considerable risks to the use of nano-drug carriers. On the other hand, such responses may also turn out to become beneficial, if only we learn how to control the carrier-induced responses of the immune system. Unfortunately, our knowledge regarding the processes involved in the interactions of the carrier with the biological milieu following in vivo administration is still limited. Our research efforts are aimed at opening this "black box" and fully understand its contents.

Microwave Hazard on Proteins Adsorbed on Carbon Nanotubes

Masahito Sano

Department of Polymer Science and Engineering, Yamagata University

4-3-16 Jyonan, Yonezawa, Yamagata 992-8510 Japan

Carbonized compounds are heated quite efficiently by microwave (MW) radiation and carbon nanotubes (CNTs) are not exceptions. For instance, a home-use MW oven, which usually operates at 1000 W or more power, heats CNTs to temperatures over the melting point of glass in seconds. This high heating efficiency has been applied to CNT chemistry. The reaction that has produced only 50% yield by heating with an ordinary oil bath for one week gives nearly 100% yield with MW heating for 30 min [1]. Because CNTs are heated much faster than other substances, those molecules close to CNTs react faster than those away from CNTs. This property has been successfully applied to produce Pt nanoparticles only on CNT surfaces for fuel cell applications [2]. The penetrating property of MW radiation into bulk materials has been demonstrated to improve viscoelastic properties of CNT-polymer composites by local heating of CNTs in the polymer matrix [3].

In these days, many electric appliances operate at MW frequencies. Mobile phones utilize MW radiation, nearly 1 W power, to communicate with the base station, which radiates about 30 W. Most computer devices operate at MW frequencies with unknown radiation outputs. In fact, we are constantly irradiated by MW radiation in every day life.

Considering extremely high heating efficiency of CNTs, it is of great importance to investigate the effects of MW radiation on biological systems co-existing with CNTs. In particular, we are interested in the maximum radiation dose for safe use. As an initial approach, we have investigated the minimum MW irradiances necessary to denature proteins adsorbed on CNTs in solution. We have examined hemoglobin first, since it is known to interact specifically with CNTs [4]. More detailed analyses using heat-resisting cytochrome c will be also presented.

[1] Kubota, K., Sano, M. and Masuko, T. Jpn. J. Appl. Phys., 44, 465-468 (2005).

[2] Yoshida, S. and Sano, M. Chem. Phys. Lett. 433, 97 (2006).

[3] Yoshida,S., Mitsumata, T. and Sano, M. Chem. Lett., 35, 262-263 (2006).

[4] Ken, K. and Sano, M. Chem. Lett., 35, 1062 (2006).

Organic Synthesis of Aluminum Silicates and their property of water vapor adsorption

Ryosuke Nakanishi[1], Masaya Suzuki[2], Keiichi Inukai[1], Masaki Maeda[1] and Hideo Hashizume[3]

[1]AIST Chubu, 2266-98 Shimoshidami, Moriyama, Nagoya, Aichi, 463-8560, JAPAN

[2]AIST Tsukuba, 1-1-1 Higashi, Tsukuba, Ibaraki, 305-8567, JAPAN

[3]NIMS, 1-1 Namiki, Tsukuba, Ibaraki, 305-0044, JAPAN

Energy conservation is very important from the standpoints of CO_2 emission limitation and preservation of natural resources. Adsorption and desorption of water bring heat transfer, and this also leads to energy saving when the heat is used effectively. Aluminum silicate such as zeolite, allophone and imogolite has small pores and high affinity of water. They are expected to be used as desiccant and heat pump materials.

In the process of synthesis using aluminum tri-sec-butoxide and tetraethoxysilane, we found out the compounds having the high water vapor adsorption ability at the middle relative water vapor pressures. Especially, they have excellent water vapor adsorption ability at the Si/Al ratio of 1.2 and 1.5. Adsorbed water content were around 60~70 wt.% and 100~120 wt.% when the relative humidity were 60 % and 95 %, respectively. Adsorbed water content increased linearly. These aluminum silicates gave nine sharp XRD peaks (15.4°, 19.3°, 20.5°, 22.7°, 23.8°, 25.5°, 26.7°, 27.9° and 29.2°) until 2θ = 30.0° at room condition (20℃, 40 %RH). Some of these peaks gradually weakened as temperature of XRD measurement environment increased (20~90℃). Finally the strong peak at 2θ = 22.7° and small peaks at around 2θ = 26.7° and 27.9° remained at more than 70℃ (Fig. 1). Intensity of the peak at 2θ = 22.7° increased at more than 50℃. Keeping humidity of 5 % for 48h, these peaks didn't disappear. This may indicate that water vapor (H_2O) aligned and make crystal layer at 20-60℃ and this layer disappeared more than 70 ℃ by heating. Pore-size distribution and pore volume of these aluminum silicates by N_2 adsorption could be cleared by presentation.

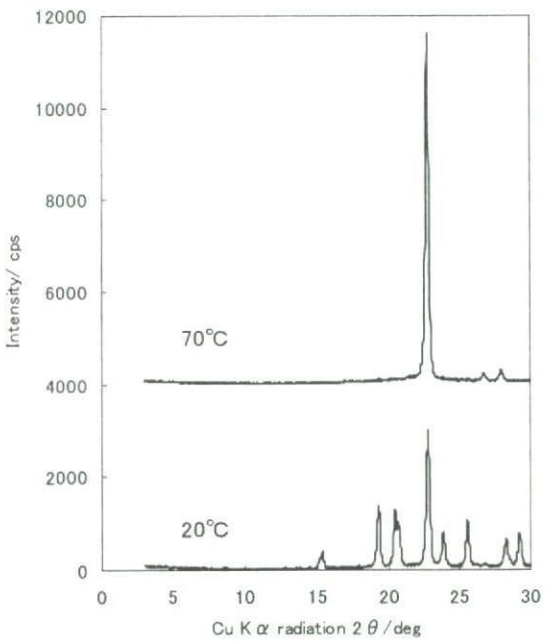

Fig. 1 XRD patterns of the aluminum silicate (Si/Al = 1.2) at measured temperature 20℃ (below) and 70℃ (above).

Magnetic Nanoparticles for Magnetic Hyperthermia

S. Aizawa[1], T. Hosono[1], Y. Sato[1], K. Tohji[1] and B. Jeyadevan[1]

[1]6-6-20 Aoba, Aramaki, Aoba-ku, Sendai, 980-8579 Japan

Graduate School of Environmental Studies, Tohoku University

Magnetic hyperthermia is considered as one of the superior alternative therapeutical method for cancer. The heat absorption rate of the magnetic nanoparticles seriously depends on their size and size distribution. Theoretical calculation results demonstrated that monodispersed magnetite nanoparticles with their diameter ranging between 11-13 nm are suitable for hyperthermia applications. In this paper, we discuss about oxidation and pH controlled coprecipitation synthesis techniques to obtain the same.

Recently, we reported that magnetic nanoparticles with the diameters of 13, 14 and 19 nm was successfully synthesized by utilizing the traditional oxidation method, and that aqueous suspension of magnetite particle with average diameter of 13 nm exhibited highest temperature (T_h) of 76 °C in 600 s when it exposed to AC magnetic field (3.2 kA/m and 600 kHz) as shown in Fig. 1. However, the particles size distribution synthesized by traditional method was wide because of inhomogeneous nucleation resulting from the fluctuation in the hydroxyl ion concentrations during synthesis. Consequently, T_h becomes relatively lowered.

Therefore, we tried to restrict the fluctuation of pH by utilizing buffer solution during the particle synthesis at pH 9.5, 10.0, 10.6, and 11.2 (90 °C). As a result, particle size distribution become narrower and average particle sizes were 14, 13, 13 and 12 nm, respectively. The highest T_h of 93 and 63 °C were recorded for the suspensions dispersing particles synthesized at pH 9.5 and 11.2, respectively (Fig. 1). Lower heating rate of the particles synthesized at higher pH was confirmed due to smaller particle size. Details on the synthesis of MP with narrower size distribution and their magnetic and heating properties will be also reported.

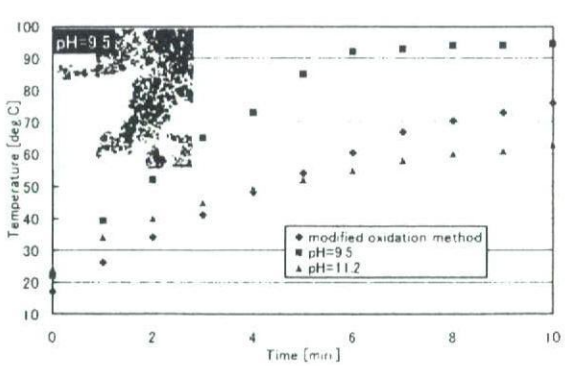

Fig.1 Change in the temperature of the suspensions as the function of particle size and distribution. AC magnetic field strength and frequency was 3.2 kA/m and 600 kHz, respectively

Microstructure and Surface Characteristics of Anodized and Hydrothermal Treated Titanium

IL SONG PARK[1,2], MAN HYUNG LEE[2], MIN HO LEE[1], KYEONG WON SEOL[2], TAE SUNG BAE[2*], FUMIO WATARI[3]

[1]Dept. of Dental Biomaterials and Oral Bioscience, Scholl of Dentistry, Chonbuk National University, Jeonju, South Korea, 561-756

[2]Division of Advanced Materials Engineering and Research Center of Industrial Technology, Engineering College, Chonbuk National University, Jeonju, South Korea, 561-756

[3]Biomedical, Dental Materials and Engineering, Dept. of Oral Health Science, Graduate School of Dental Medicine, Hokkaido University, Sapporo, Japan, 060-8586

Objectives. Titanium is widely used as an implant material because of the excellent biocompatibility of titanium oxide layer [1]. However, natural surface oxide may contain a large number of defects and have bioinert surface [2]. To increase a bioactivity of titanium surface, anodic spark oxidation method was applied in this study. We evaluated microstructure and surface characteristics to investigate the effect of anodization and hydrothermal treatment on the titanium surface.

Materials and Methods. Two types of mixtures of 0.02M-GP (Glycerolphosphate disodium salt) + 0.2M-CA (Calcium acetate) and 0.02M-GP + 0.3M-CA were used as an electrolyte. By increasing the anodizing voltage to 220V, 260V, 300V, and 360V, the effects of the anodizing voltage were examined by evaluating the surface morphology and properties after anodization and a hydrothermal treatment.

Results and Discussion. In this study, a dense and stable oxide layer with micropores was formed by anodic spark oxidation on pure titanium surface and hydroxyapatite crystals were formed by hydrothermal treatment. Breakdown voltage varied from 230V to 210V with the anodizing voltage. As the voltage increased after breakdown, the pore size increased. After the hydrothermal treatment, the amount of HA crystal precipitation was also increased as the voltage increased. In addition, the minute HA crystals with several and several tens of nanometers were observed on the oxide surface after hydrothermal treatment. The mean surface roughness (Ra) of the anodizing surface was also increased with the voltage. It is thought that existence of HA crystal and rough surface are good for mechanical bond strength and bioactivity [3].

Literature References

[1] B. Kasemo: J. Prosthet. Dent. Vol 49 (1983) p 832

[2] B. Kasemo, and J. Lausmaa: Quintessence Publishing. (1985) p 99

[3] C. Larsson, P. Thomsen, B.O. Aronsson, M. Rodahl, J. Lausmaa, B. Kasemo, and L.E. Ericson: Biomaterials Vol. 17 (1996) pp 605-616

Synthesis and characteristics of silver sulfide stratified photocatalyst

Yohei Baba, Tsugumi Hayashi, Toshiharu Taga,

Hideyuki Takahashi, and Kazuyuki Tohji

6-6-20 Aoba, Aramaki, Aoba-ku, Sendai, 980-8579 Japan

Graduate School of Environmental Studies, Tohoku University

The development of clean energy has vigorously studied since fossil fuels are depleted and global warming becomes significant. Sulfide type photocatalyst, which can produce hydrogen energy from hydrogen sulfide (H_2S) under light irradiation, has the possibility for the energy conversion from natural energy (solar energy) into clean energy (hydrogen), moreover it can remove the harmful H_2S gas.

Recently, we reported that zinc sulfide (ZnS) and/or cadmium sulfide (CdS) photocatalyst particles with specific morphology, called as stratified structure, can induce H_2S splitting very efficiently. However, former can utilize only under UV-light irradiation, and the use of later is limited due to its toxicity. Therefore, we should select the other photocatalyst which act under wide wavelength light irradiation and has non-toxicity, such as silver sulfide (Ag_2S), as a new H_2S splitting photocatalyst material.

Morphology and crystal phase of precursor materials (metal oxide and/or hydroxide) was seriously affected to that of stratified type photocatalyst. Moreover, the size of materials was affected to the activity. Therefore, in this study, Ag_2O nanoparticles were tried to synthesize as the function of metal concentration in solution, additional rate of PVP/PVA, and pH. Figure 1 shows SEM images of synthesized Ag_2S precursor particles sulfrized by (a) Na_2S without PVA, (b) thiourea without PVA, (c) Na_2S with PVA addition, and (d) thiourea with PVA addition. As shown in figure, particle size and morphology can be controlled by the additional amount of surfactants (PVA and PVP) and sulfurizing agent. The results of photocatalytic activity (Fig.2) showed that it was seriously affected by the particle size and surface condition by PVP/PVA adsorption.

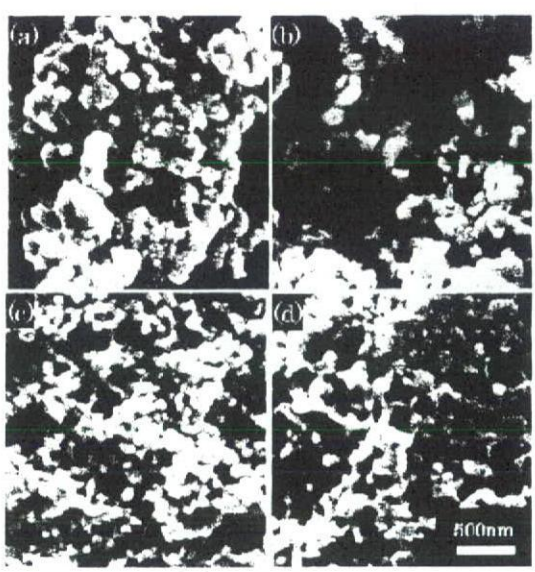

Fig.1 SEM images of synthesized Ag_2S particles

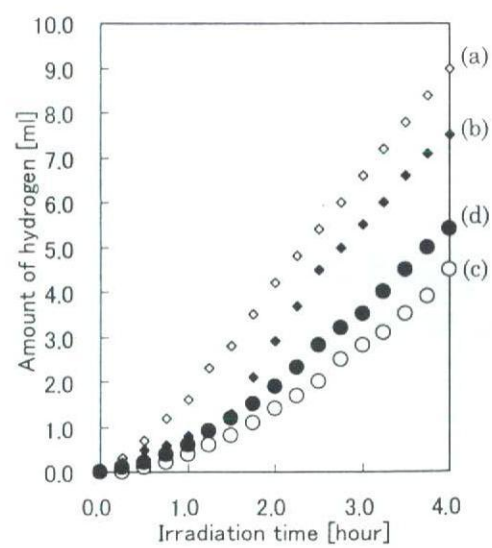

Fig.2 Photocatalytic activity of synthesized Ag_2S particles evaluated by hydrogen evolution rate in the H_2S alkaline solution under UV light irradiation